Medical Research Archives

European Society of Medicine

OPEN ACCESS

Published: December 31, 2023

Citation: Ratti, V. and Wallace, D., 2023. Dilution Effect of the Refractory Lizard Host on the Transmission of the Lyme Disease Pathogen by Its Tick Vector in Northern California. Medical Research Archives, [online] 11(12). https://doi.org/10.18103/mra.v11i12.4948

DOI: https://doi.org/10.18103/mra.v11i12.4948

ISSN: 2375-1924

RESEARCH ARTICLE

Dilution Effect of the Refractory Lizard Host on the Transmission of the Lyme Disease Pathogen by Its Tick Vector in Northern California

Vardayani Ratti[1] and Dorothy Wallace[2*]

[1]California State University Sacramento, CA, USA
[2]Dartmouth College, NH, USA

[*]dwallace@math.dartmouth.edu

ABSTRACT

A current model for *Ixodes scapularis* was revised and extended to represent the temperature dependent life cycle and host structure for *Ixodes pacificus*, the vector of the Lyme disease pathogen *Borrelia burgdorferi* in the Western United States. Parameters were adjusted to reflect data collected in Mendocino, CA. The hosts for *I. pacificus* include the Western Fence Lizard, which is not only an incompetent host for *B. burgdorferi*, but some studies claim that it eliminates it in ticks that feed on this lizard, making it an example of a so-called refractory host. The lizard host has been proposed as a reason for lower prevalence of Lyme disease in the West than in the northeast. This hypothesis was tested quantitatively by varying the number of lizard hosts. When refractory host densities are comparable to those reported for Mendocino County, CA, Resulting disease risk is lowered roughly in proportion to the total questing infected nymph population, and that proportion corresponds to the ratio of Lyme disease prevalence in Mendocino to that of the northeast. Model results suggest that the presence of refractory hosts produces a dilution effect for *B. burgdorferi* infection and is likely to be the reason for observed lower prevalence of Lyme disease in the Western United States.

Introduction

Lyme disease is a vector-borne disease of increasing concern. The disease is transmitted by ticks and maintained in the wild by a range of reservoir hosts. In the West, the relevant tick species is *Ixodes pacificus*, or the Western black-legged tick. The life cycle of this tick includes three stages: larva, nymph, and adult. These stages are punctuated by feeding cycles consisting of a questing period, in which ticks emerge to find a host, and a feeding period on that host[1–3]. Off host intervals offer time for maturation, which is a temperature-dependent process[4–6].

Hosts of the vector *I. pacificus* include birds, mammals, and lizards[7–9]. Hosts may be described as "competent," or able to be a disease reservoir; "incompetent," or unable to carry the disease; or, in the special case of the Western fence lizard, "refractory." MacDonald et al. and others argue that the composition of host species determines the risk of Lyme disease in California, through studying habitat suitability of several small mammal host species that serve as disease reservoirs and comparing these with spatial human disease data[10–13]. Statistical geospatial techniques have combined host data with temperature constraints to produce habitat suitability maps for *I. pacificus*[14]. The Western Fence Lizard (*Sceloporus occidentalis*) is a major host for *I. pacificus* in the West[15]. An unusual aspect of this host is its purported ability to eliminate *B. burgdorferi* in the gut of feeding nymphs, thereby reducing the probability of transmission of disease during the subsequent adult feeding[16–18]. This lizard is described as a "refractory host."

Mendocino county in California is the site of ongoing tick data collection, resulting in multiple published descriptions of data, including distribution, questing activity, and seasonal patterns[19–22]. The use of Mendocino as a test area for this study is further justified because it is a relatively high-risk area for Lyme disease in California[23].

This study quantifies the effects of the presence of a refractory host by varying the refractory host population using the process-based model and tracking the cumulative number of infected questing nymphs over the course of a year[24–26]. The model used is based on a prior model of *Ixodes scapularis*, the *B. burgdorferi* host in the Northeast U.S. The model was adjusted to reflect the temperature and daylength of Mendocino county[19]. Maturation responses to temperature and daylength were also adjusted to produce a seasonal distribution of questing nymphs similar to data from Mendocino. Finally, the model is adjusted to include the refractory host and uses estimated host densities for the Mendocino area[15,27]. As the number of questing nymphs is far larger than the number of questing adults, disease risk from infected questing nymphs is larger than for adults and is the quantity tracked in this study.

If feeding ticks are very likely to find an incompetent reservoir host, then disease transmission in either direction would be impossible during that feeding. Thus, a large population of such hosts could result in lower numbers of infected questing ticks overall, thus reducing disease risk to humans, a hypothesis called the "dilution effect." The presence of a refractory host would be even more effective at reducing risk. Conversely, having more hosts of any sort would increase the overall population of ticks, possibly resulting in higher disease risk, a hypothesis referred to as "amplification." Dilution and amplification effects have been proposed for *B. burgdorferi* transmission for both incompetent reservoir hosts such as deer and for the refractory host[28,29]. Some have attributed dilution effects to host diversity in general[30,31].

The resulting numerical simulations are used to demonstrate that the model produces an accurate seasonal description of questing nymph data in Mendocino. It further tests the hypothesis that the presence of the refractory host produces the low risk of Lyme disease compared to risk in the Northeast U.S. The simulation is then revised by lowering the number of refractory hosts and tracking both the total number of questing nymphs and the number of infected questing nymphs over one year.

Methods

The process-based model for tick population dynamics and disease dynamics is illustrated in Figure 1. Each compartment in the diagram corresponds to one of the differential equations governing the model. Temperature dependent transitions are shown by orange arrows and temperature independent transitions by blue arrows. Infection of ticks feeding on infected hosts are shown by the red arrows. Elimination of disease in infected ticks feeding on the refractory host is shown by the green arrow. Death processes not illustrated. Host population and disease dynamics for five classes of host: Deer (IM), Reservoir incompetent small mammals (IS), Refractory lizard host (R), Reservoir competent small mammals, both uninfected (CU) and infected (CI).

Figure: 1

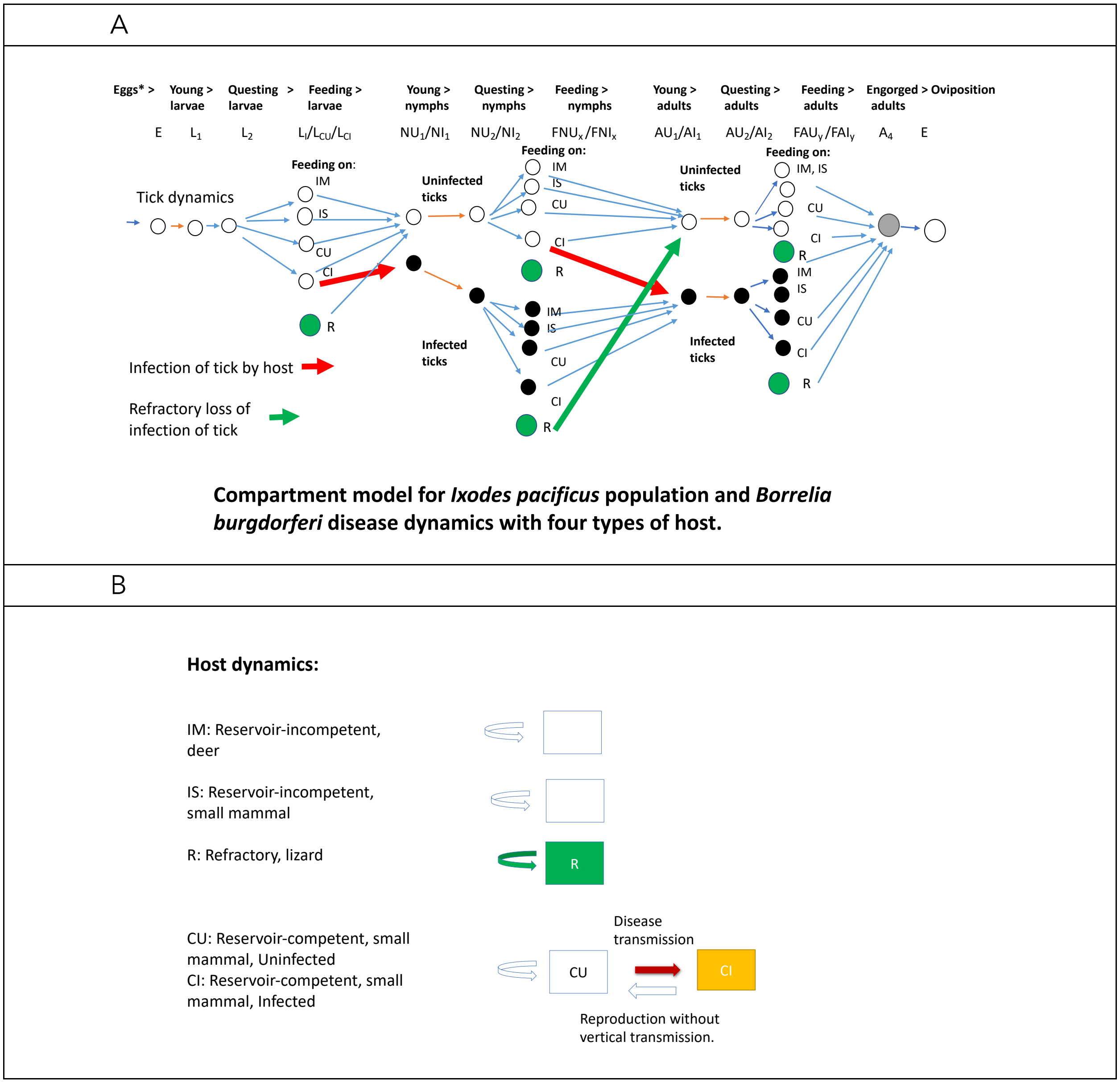

Figure 1: Compartment process diagram for system. (A) Tick population and disease dynamics are shown across the top. Temperature dependent transitions are shown by orange arrows and temperature independent transitions by blue arrows. Infection of ticks feeding on infected hosts are shown by the red arrows. Elimination of disease in infected ticks feeding on the refractory host is shown by the green arrow. Death processes not illustrated. (B) Host population and disease dynamics in the lower right, for five classes of host: IM, IS, R, CU, and CI. Death processes not illustrated.

Model development

Ticks are tracked from egg through three temperature-dependent maturation intervals punctuated by questing activity and feeding periods on hosts. Feeding ticks are tracked according to what type of host they are on and whether the host is infectious or not. They are further sorted as to their own infectious status. Incompetent hosts are separated into deer versus other smaller mammals. The refractory host represents the Western Fence lizard. The population of ticks in this model is controlled by the ability of questing ticks to find a host. There are two simplifying assumptions worth noting. First, any tick stage may feed on any type of host, with ticks allocated according to host density and on-host carrying capacities. That is, there is no host preference for different tick stages in this model. Second, the on-host carrying capacity for each type of host restricts the numbers of on-host nymphs and adults, but not the number of feeding larvae, as these are quite small. Auxiliary equations govern the dependencies of maturation on temperature and daylength to simulate the seasonal distribution seen in data. A full set of equations is given in Appendix A.

Parameter estimates

Model parameters are based on numerous sources and, when possible, matched to the Hopland area of Mendocino, CA. Default parameters that have not been changed from a prior model are those of Wallace et al.[24] Adjusted parameters address differences in annual temperature patterns, host densities and on-host tick carrying capacities, and the observed summer diapause in the seasonal patterns of tick abundance. A table of parameters is given in Appendix A.

TEMPERATURE, DAYLENGTH, AND DEPENDENCE ON THESE

A truncated Fourier series was fit to reanalysis data for mean daily temperature for Mendocino (cite KNMI). Reanalysis refers to a hybrid product combining station data, satellite data and weather models. Two years (730 days) of data for the cell with grid corners in Mendocino (lon = -123.625 -123.375, lat = 39.375 39.625), starting January 1, 2020. Mean daily temperature was calculated as the average of reported minimum and maximum daily temperatures. The resulting estimate was adjusted to have a 365 day periodicity.

Troughton and Levin compared the life cycles of several tick species[5]. *I. scapularis* and *I. pacificus* had stages of comparable length, each within the error bars for the other. Based on this comparison, *I. pacificus* stages were taken to be the same as those of *I. scapularis* in a prior model for that species[24]. Temperature dependence of maturation stages were also taken to have the same form, derived from experiments by Ogden et al.[32] However, the peak maturation rate was revised to 15 deg Centigrade to reflect time series data in Eisen et al.[19]

Questing behavior is often suspended for periods, sometimes referred to as "diapause." Temperature, humidity, and daylength have all been proposed as reasons for this suspension[4,19,33–36]. Quiescence or diapause based on temperature and daylength were used to approximate the time series for observational data of questing nymphs in Eisen et al.[19]

Eisen et al note that no questing is observed below 10 deg C. The model was adjusted with a Heaviside term preventing ticks from passing into the questing stage below that temperature. Similarly, ticks were not observed questing during the hottest part of summer. It is not clear whether high temperature or low humidity or some other factor is the cause of this diapause or quiescence, so temperature was used as a convenient proxy. In the model, another Heaviside cutoff at 15 deg C was used to suppress questing above this temperature. Finally, no autumnal questing was reported. A third Heaviside function based on daylength was used to suppress late year questing when daylength is less than 0.45 (about 11 hours).

HOST DENSITIES AND ON-HOST TICK CARRYING CAPACITIES

A wide range of reptiles, birds and mammals may host *I. pacificus*[8]. A subset of these was chosen to represent hosts based on density estimates by Casher et al for small vertebrates in chaparral of the Hopland area of Mendocino County, CA. (7800 small mammals per km^2, 14600 Western fence lizards per km^2)[15]. Deer estimates are based on 2014 black-tailed deer density estimates for Mendocino National Forest (46 per km^2)[27]. On-host tick capacities are not reported for these hosts and are taken from measurements of similar hosts for *I. scapularis*[24]. Avian hosts are omitted from the model because it is believed they do not contribute significantly to local transmission dynamics[2]. Mammal hosts of *I. pacificus* that are not competent hosts for *B. burgdorferi* probably are present but have not been assessed either for population density, on-host tick carrying capacity or susceptibility to infection. Some hosts, such as opossum, also occur on in the Eastern U.S. The population density of such incompetent hosts and their parameters have been drawn from the prior model[24].

Numerical experiments

Simulations were run to day 3000 to observe steady state behavior of the system. Day 2555 to day 2920 represents year 8 of the simulation. Default parameters are provided in Appendix A. For Figure 4, the carrying capacity for the refractory host was altered from 100 to the default value. All calculations were done using Matlab ODE solver[37].

Results

The model with default parameters given in Appendix A produces a seasonal pattern of questing ticks that begins around April 1 and concludes around July 1. The maximal number of questing nymphs produced is between 2.5*10^5 and 3*10^5 per km^2. Figure 2 shows the associated daylength (2A), temperature (2B), questing nymphs in year 8 (2C) and all questing stages (2D). A slight bimodal pattern is seen for questing nymphs (2C).

Figure: 2

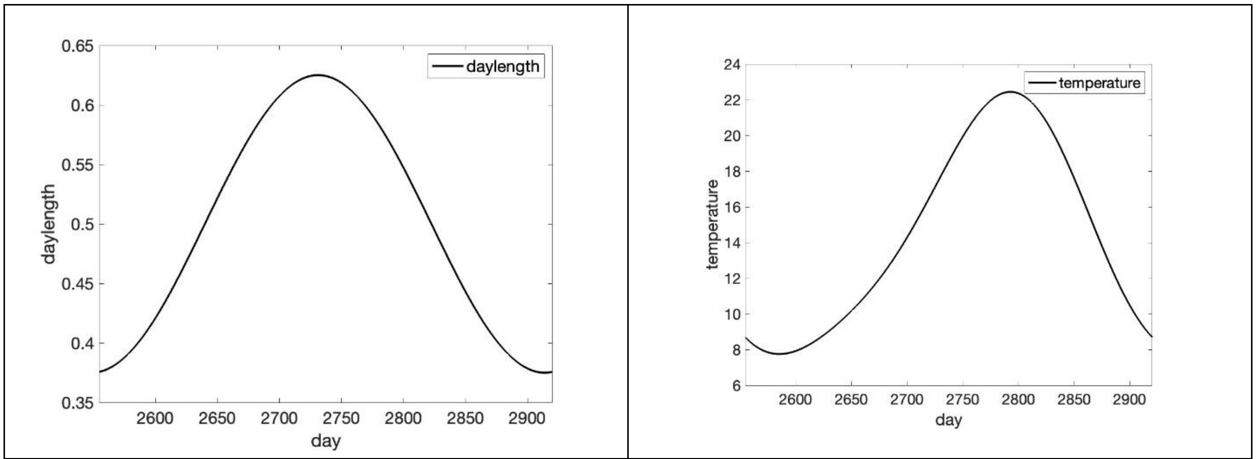

A Daylength for Mendocino CA

B Temperature for Mendocino CA

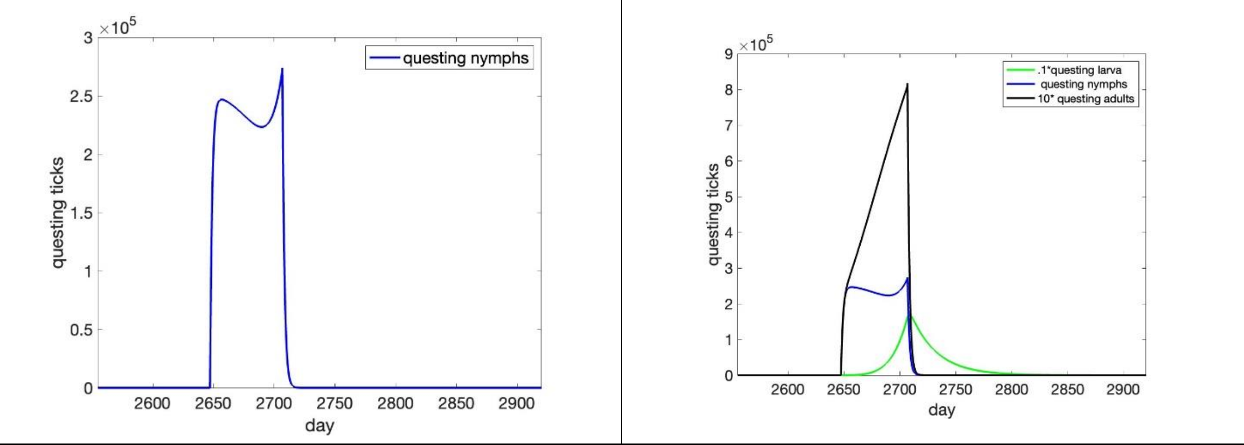

C Abundance of questing nymphs

D Abundance of questing ticks, all stages

Figure 2: Model behavior for default parameters, day 2555 to day 2920, representing year 8 of the simulation. A) Day length for Mendocino, CA. Questing is suppressed in the model when daylength is below 0.45 days. B) Average daily temperature for Mendocino, CA. Questing is suppressed for temperatures below 10 deg C or above 15 deg C. C) Abundance of questing nymphs for year 8. Questing nymphs are present from approximately April 1 to July 1, with abundance ranging from $2.5*10^5$ to $3*10^5$ per km^2 during that period. D) All questing stages in year 8. Note that questing larvae are scaled by 0.1 and questing adults are scaled by 10.

Figure 3 separates infected nymphs from the total questing populations. In Figure 3A the infected questing nymph population is seen to be quite low compared to the total questing nymph population. In Figure 3B the percentage of questing nymphs that are infected is shown to be approximately 1.5% of total questing nymphs. This percentage gives a maximum of approximately $4.5*10^3$ infected questing nymphs per km^2.

Figure: 3

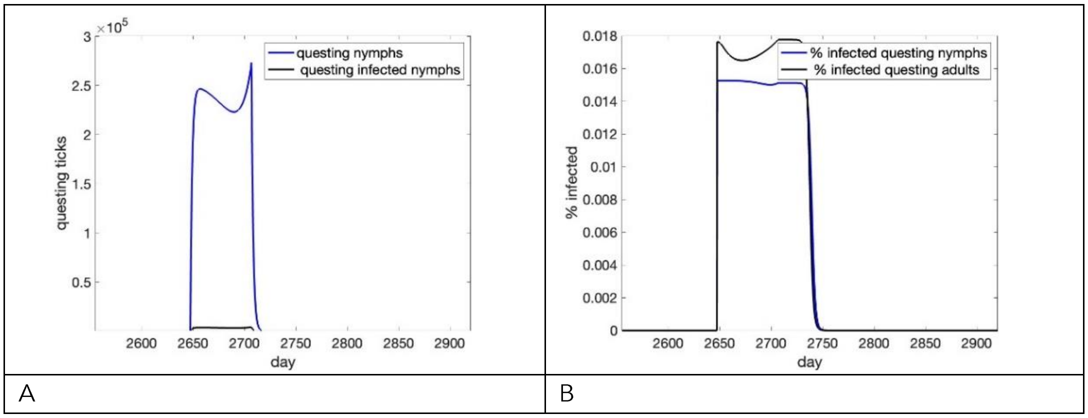

A

B

Figure 3: Model runs for year 8 showing A) total questing nymphs and infected questing nymphs, and B) percent infected questing nymphs and adults.

Figure 4 shows the consequences of changing the number of refractory hosts for both cumulative questing total and infected ticks, holding all other host populations constant at default levels. Comparison of infected and total questing ticks illustrates the dilution effect of the refractory host. As more refractory hosts are available, total tick populations rise but infected tick populations drop.

Figure: 4

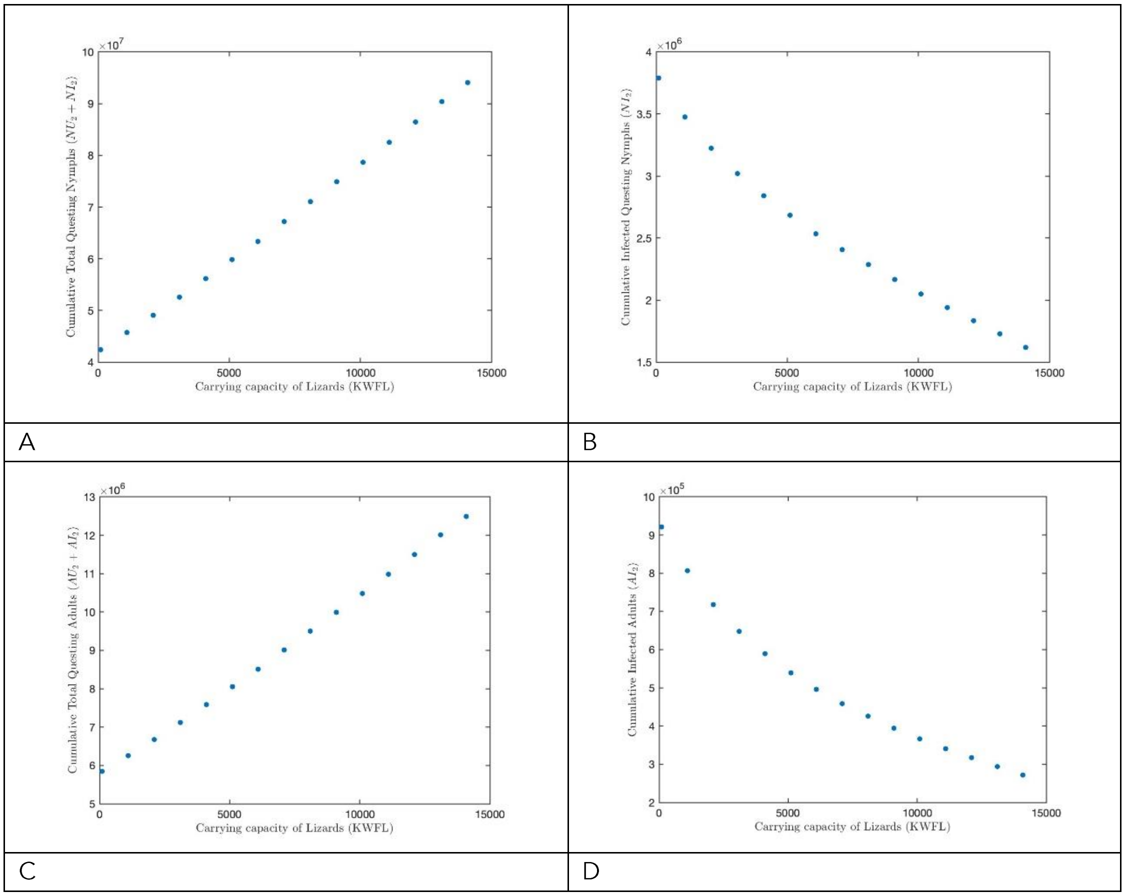

A

B

C

D

Figure 4: Cumulative questing ticks over the last year of the simulation, for various populations of the refractory host, Western Fence Lizard, as determined by carrying capacity for this host (KWFL). (A) Cumulative questing nymphs, (B) Cumulative infected questing nymphs, (C) Cumulative questing adults, and (D) Cumulative infected questing adults.

Discussion

The data given in Eisen et al,[19] for 1998 to 2001, show a seasonal pattern of questing nymphs that ranges from around April 1 through July, with low values in July. The model runs shown in Figure 1 are having a somewhat shorter seasonality, ending around July 1. However, most of the ticks found in the Eisen et al study were present during this period. The maximum abundance of questing ticks observed ranged from 3 to 7 ticks per 100 m^2, which is $3*10^5$ to $7*10^5$ ticks per km^2. The model predicts a maximum of approximately $2.5*10^5$ ticks per km^2, slightly below the observed maximum but still of the same general magnitude.

DISEASE RISK COMPARISON WITH NORTHEASTERN U. S.

Model predictions shown in Figure 3 yield a maximum of approximately $4.5*10^3$ infected questing nymphs per km^2. This number can be compared with model estimates for *I. scapularis* of a maximum of $12*10^4$ infected question nymphs per km^2 [24].

The percentage of questing nymphs that are infected in the simulation with default parameters is approximately 1.5%. This answer compares favorably with the 0.6% to 9.9% reported for the Western U.S[2,38].

The average incidence rate of Lyme disease in California per 100,000 people is reported to be between 0.1 and 0.9, while in the northeast U.S. has been as high as 83[2]. In some northern counties, where there is a higher abundance of *I. pacificus*, the rate is currently as high as 4 cases per 100,000 people (cdph). At its highest, the ratio of the incidence rates for California to the Northeastern U.S. is approximately 0.036 (taking the Northern California rate as 3). As the abundance of infected ticks should be correlated with disease risk, we can compare the ratio of $4.5*10^3$ infected questing *I. pacificus* nymphs, produced by this simulation with default parameters, with the prior estimate of $12*10^4$ peak infected nymphs for *I. scapularis*, which yields a ratio of 0.0375[24]. Both models and data show that disease risk is much lower in the Western than in the Northeastern U.S, by a factor of less than 0.04. Actual disease risk is, however, a local property depending on host distribution, human population density, weather, and other factors[11,39,40].

DILUTION EFFECT OF WESTERN FENCE LIZARD

It is clear from simulations shown in Figure 4 that the refractory host produces a strong dilution effect. This result is in contrast to simulations of *I. scapularis* that only include incompetent reservoir hosts, where dilution effects are only seen at extremely low populations of competent reservoir hosts[26]. Swei et al tested lizard removal in a plot of land in Marin County[41]. They found that, although the prevalence of infection increased in questing nymphs, the absolute numbers of questing nymphs went down enough to compensate for this, and the authors concluded that increased lizards were more likely to amplify rather than dilute disease. It must be noted, however, that the lizard removal study was for a single year. The life cycle of ticks spans several years, and disease dynamics follow more slowly than that. The simulations in this study allow the system to reach steady state, which takes a few virtual years. During a multi-year period of feeding on competent reservoir hosts, the prevalence of infection is likely to rise further in both ticks and hosts.

FURTHER DIRECTIONS

As with all models, the one used in this study could be improved and extended. Tick host inventories and on-host tick burdens could be more thoroughly measured and in different regions. The model itself could perhaps be modified to take host preference into account in some way, as was done in a prior study of *I. scapularis*[26]. In that study host preference did not make much difference in the question of dilution/amplification effects, but maybe it would make a difference here.

The temperature model used for Mendocino could also be improved. Temperatures are not the same from year to year and daily variation from the seasonal norm could be included, using methods like those of Benth et al.[42] Humidity is not directly taken into account yet in the model, and this improvement awaits laboratory investigations into the coupled effects of temperature and humidity on tick maturation rates and questing behavior.

Finally, the model could be extended to include interventions that reduce tick populations or environmental changes that could either reduce or increase tick populations, with a view to predicting changes that may result.

Conclusion

A simulation was constructed based on the biology of the life cycle of *I. pacificus* and disease transmission of *B. burgdorferi*, including the refractory host, *S. occidentalis*. The simulation approximately reproduces the seasonal pattern of tick questing as well as the estimated numbers of questing ticks in Mendocino, CA. The predicted ratio of maximum infected questing *I. pacificus* nymphs in Mendocino to maximum infected questing *I. scapularis* nymphs in the Northeastern U.S. is shown to be comparable to the corresponding ratio of Lyme disease cases in the human populations. Simulations predict that, as the population of S. occidentalis is reduced, the overall questing nymph populations are reduced but the infected questing nymph populations rise, indicating that the Western Fence lizard produces a dilution effect for *B. burgdorferi* infection in ticks, and corresponding dilution of risk to humans.

Conflicts of Interest Statement:

None

Funding Statement:

This study was funded in part by the National Science Foundation (award 2019609).

Acknowledgements Statement:

The authors wish to thank Mike Teglas, Department of Agriculture, Veterinary and Rangeland Sciences, Univ. of Nevada, Reno, for valuable discussions.

References:

1. McVicar M, Rivera I, Reyes JB, Gulia-Nuss M. Ecology of Ixodes pacificus ticks and associated pathogens in the Western United States. *Pathogens*. 2022; 11(1):89. doi:10.3390/pathogens11010089

2. Dizon C, Lysyk TJ, Couloigner I, Cork SC. Ecology and epidemiology of Lyme disease in Western North America. *Zoonotic Dis.* 2023; 3(1):20–37. https://doi.org/10.3390/zoonoticdis3010004

3. Maggi RG, Toliver M, Richardson T, Mather T, Breitschwerdt EB. Regional prevalences of Borrelia burgdorferi, Borrelia bissettiae, and Bartonella henselae in Ixodes affinis, Ixodes pacificus and Ixodes scapularis in the USA. Ticks Tick Borne Dis. 2019; 10(2):360-364. doi: 10.1016/j.ttbdis.2018.11.015

4. Padgett KA, Lane RS. Life cycle of Ixodes pacificus (Acari: Ixodidae): timing of developmental processes under field and laboratory conditions. *J Med Entomol*. 2001; 38(5):684–693. doi:10.1603/0022-2585-38.5. 684

5. Troughton DR, Levin ML. Life cycles of seven ixodid tick species (Acari: Ixodidae) under standardized laboratory conditions. *J Med Entomol*. 2007; 44(5):732–740. doi:10.1603/0022-2585(2007)44[732:lcosit]2.0.co;2

6. Peavey CA, Lane RS. Field and laboratory studies on the timing of oviposition and hatching of the western black-legged tick, Ixodes pacificus (Acari: Ixodidae). *Exp Appl Acarol*. 1996; 20(12):695–711. doi:10.1007/BF00051555

7. Eisen L, Eisen RJ, Lane RS. The roles of birds, lizards, and rodents as hosts for the western black-legged tick Ixodes pacificus. *J Vector Ecol*. 2004; 29(2):295–308.

8. Castro MB, Wright SA. Vertebrate hosts of Ixodes pacificus (Acari: ixodidae) in California. *J Vector Ecol*. 2007; 32(1):140–149. doi:10.3376/1081-1710(2007)32[140:vhoipa]2.0.co;2

9. Westrom DR, Lane RS, Anderson JR. Ixodes pacificus (Acari: Ixodidae): population dynamics and distribution on Columbian black-tailed deer (Odocoileus hemionus columbianus). *J Med Entomol*. 1985;22 (5):507–511. doi:10.1093/jmedent/22.5.507

10. MacDonald AJ, Hyon DW, Brewington JB, O'Connor KE, Swei A, Briggs CJ. Lyme disease risk in southern California: abiotic and environmental drivers of Ixodes pacificus (Acari: Ixodidae) density and infection prevalence with Borrelia burgdorferi. *Parasit Vectors*. 2017;10(1):1–6. Published 2017 Jan 5. doi:10.1186/s13071-016-1938-y

11. MacDonald AJ, McComb S, Sambado S. Linking Lyme disease ecology and epidemiology: Reservoir host identity, not richness, determines tick infection and human disease in California. *Environ Res Lett*. 2022; 17(11). DOI 10.1088/1748-9326/ac9ece

12. Salkeld DJ, Lane RS. Community ecology and disease risk: lizards, squirrels, and the Lyme disease spirochete in California, USA. *Ecology*. 2010; 91(1):293–298. https://doi.org/10.1890/08-2106.1

13. Salomon J, Lawrence A, Crews A, Sambado S, Swei A. Host infection and community composition predict vector burden. *Oecologia*. 2021; 196(2):305-316. https://doi.org/10.1007/s00442-021-04851-9

14. Hahn MB, Feirer S, Monaghan AJ, et al. Modeling future climate suitability for the western blacklegged tick, Ixodes pacificus, in California with an emphasis on land access

and ownership. *Ticks Tick Borne Dis*. 2021; 12(5):101789. doi:10.1016/j.ttbdis.2021.101789.

15. Casher L, Lane R, Barrett R, Eisen L. Relative importance of lizards and mammals as hosts for ixodid ticks in northern California. *Exp Appl Acarol*. 2002; 26(1-2):127-143. doi: 10.1023/a:1020911306291

16. Lane RS, Loye JE. Lyme disease in California: interrelationship of Ixodes pacificus (Acari: Ixodidae), the western fence lizard (Sceloporus occidentalis), and Borrelia burgdorferi. *J Med Entomol*. 1989; 26(4):272-278. doi:10.1093/jmedent/26.4.272

17. Lane RS, Quistad GB. Borreliacidal factor in the blood of the western fence lizard (Sceloporus occidentalis). *J Parasitol*. 1998; 84(1):29-34.

18. Lane RS, Mun J, Eisen L, Eisen RJ. Refractoriness of the western fence lizard (Sceloporus occidentalis) to the Lyme disease group spirochete Borrelia bissettii. *J Parasitol*. 2006;92(4):691-696. doi:10.1645/GE-738R1.1

19. Eisen L, Eisen RJ, Lane RS. Seasonal activity patterns of Ixodes pacificus nymphs in relation to climatic conditions. *Med Vet Entomol*. 2002;16(3):235-244. doi:10.1046/j.1365-2915.2002.00372.x

20. Eisen RJ, Eisen L, Lane RS. Predicting density of Ixodes pacificus nymphs in dense woodlands in Mendocino County, California, based on geographic information systems and remote sensing versus field-derived data. *Am J Trop Med Hyg*. 2006;74(4):632-640.

21. Eisen RJ, Clark RJ, Monaghan AJ, Eisen L, Delorey MJ, Beard CB. Host-seeking phenology of Ixodes pacificus (Acari: Ixodidae) nymphs in Northwestern California in relation to calendar week, woodland type, and weather conditions. *J Med Entomol*. 2017;54(1):125-131. doi:10.1093/jme/tjw155

22. Tälleklint-Eisen L, Lane RS. Variation in the density of questing Ixodes pacificus (Acari:Ixodidae) nymphs infected with Borrelia burgdorferi at different spatial scales in California. *J Parasitol*. 1999; 85(5):824–831.

23. Rose I, Yoshimizu MH, Bonilla DL, Fedorova N, Lane RS, Padgett KA. Phylogeography of Borrelia spirochetes in Ixodes pacificus and Ixodes spinipalpis ticks highlights differential acarological risk of tick-borne disease transmission in northern versus southern California. *PLoS One*. 2019; 14(4):e0214726. Published 2019 Apr 4. doi:10.1371/journal.pone.0214726

24. Wallace D, Ratti V, Kodali A, et al. Effect of rising temperature on Lyme disease: Ixodes scapularis population dynamics and *Borrelia burgdorferi* transmission and prevalence. *Can J Infect Dis Med Microbiol*. 2019;2019: 9817930. Published 2019 Sep 16. doi:10.1155/2019/9817930

25. Winter JM, Partridge TF, Wallace D, et al. Modeling the sensitivity of blacklegged ticks (Ixodes scapularis) to temperature and land cover in the northeastern United States. *J Med Entomol*. 2021; 58(1):416–27. doi:10.1093/jme/tjaa179

26. Ratti V, Winter JM, Wallace DI. Dilution and amplification effects in Lyme disease: Modeling the effects of reservoir-incompetent hosts on Borrelia burgdorferi sensu stricto transmission. *Ticks Tick Borne Dis*. 2021;12 (4):101724. doi:10.1016/j.ttbdis.2021.101724

27. Wittmer HU, Forrester TD, Allen ML, Marescot L, Casady DS. Black-tailed deer population assessment in the Mendocino

National Forest, California final project report–December 2014. DOI:10.13140/2.1.3440.9764

28. Stafford III KC. Reduced abundance of Ixodes scapularis (Acari: Ixodidae) with exclusion of deer by electric fencing. *J Med Entomol*. 1993; 30:986–996. doi:10.1093/ jmedent/30.6.986

29. Levi T, Keesing F, Holt RD, Barfield M, Ostfeld RS. Quantifying dilution and amplification in a community of hosts for tick-borne pathogens. *Ecol Appl*. 2016;26:484–498. doi:10.1890/15-0122

30. Ostfeld RS, Keesing F. Biodiversity and disease risk: the case of Lyme disease. Conservation biology 2000;14, 722–728. https://doi.org/10.1046/j.1523-1739.2000.99014.x

31. Ostfeld RS. Biodiversity loss and the rise of zoonotic pathogens. *Clin Microbiol Infect*. 2009;15 Suppl 1:40–43. doi:10.1111/j.1469-0691.2008.02691.x

32. Ogden N, Lindsay L, Beauchamp G, et al. Investigation of relationships between temperature and developmental rates of tick Ixodes scapularis (Acari: Ixodidae) in the laboratory and field. *J Med Entomol*. 2004;41(4):622–633. doi:10.1603/0022-2585-41.4.622

33. Lane RS, Kleinjan JE, Schoeler GB. Diel activity of nymphal Dermacentor occidentalis and Ixodes pacificus (Acari: Ixodidae) in relation to meteorological factors and host activity periods. *J Med Entomol*. 1995;32(3): 290–299. doi:10.1093/jmedent/32.3.290

34. Gray JS, Kahl O, Lane RS, Levin ML, Tsao JI. Diapause in ticks of the medically important Ixodes ricinus species complex. *Ticks Tick Borne Dis*. 2016;7(5):992–1003. doi:10.1016/j.ttbdis.2016.05.006

35. Belozerov VN. New aspects in investigations of diapause and non-diapause dormancy types in insects and other arthropods. *Entomol Rev*. 2009;89: 127–136. https://doi.org/10.1134/S0013873809020018

36. Belozerov VN. Diapause and quiescence as two main kinds of dormancy and their significance in life cycles of mites and ticks (Chelicerata: Arachnida: Acari). *Acarina*. 2009; 17(1): 3–32.

37. MathWorks. 2016. Natick, MA.

38. Xu G, Pearson P, Dykstra E, Andrews ES, Rich SM. Human-biting Ixodes ticks and pathogen prevalence from California, Oregon, and Washington. *Vector Borne Zoonotic Dis*. 2019; 19(2):106–114. doi:10. 1089/vbz.2018.2323

39. Eisen RJ, Eisen L, Ogden NH, Beard CB. Linkages of weather and climate with Ixodes scapularis and Ixodes pacificus (Acari: Ixodidae), enzootic transmission of Borrelia burgdorferi, and Lyme disease in North America. *J Med Entomol*. 2016; 53(2):250–261. doi:10.1093/jme/tjv199

40. Eisen L, Eisen RJ, Lane RS. Geographical distribution patterns and habitat suitability models for presence of host-seeking ixodid ticks in dense woodlands of Mendocino County, California. *J Med Entomol*. 2006; 43(2):415–427. doi:10.1603/0022-2585(2006) 043[0415:gdpahs]2.0.co;2

41. Swei A, Ostfeld RS, Lane RS, Briggs CJ. Impact of the experimental removal of lizards on Lyme disease risk. Proceedings of the Royal Society B: Biological Sciences. 2011; 278(1720):2970–2978.

42. Benth JŠ, Benth FE, Jalinskas P. A spatial-temporal model for temperature with seasonal variance. *J Appl Stat*. 2007; 34(7):823–841

Refractory Host Appendix A

Table A1

Differential equations:
Eggs, E
1) dE/dt = b*A4 – me*metemp*E – de*E

Hardening larvae, L1
2) dL1/dt = me*metemp*E – d1*L1 – m1*L1

Questing larvae, L2
3) dL2/dt = m1*L1 – d2*L2 – m2*L2

Feeding larvae on Host type a-g, L3a- L3g
4) dL3a/dt = m2*L2*Fa*Qa – P3f*L3a – m3a*L3a
5) dL3b/dt = m2*L2*Fb*Qb – P3b*L3b – m3b*L3b
6) dL3c/dt = m2*L2*Fc*Qc – P3c*L3c – m3c*L3c
7) dL3d/dt = m2*L2*Fd*Qd – P3d*L3d – m3d*L3d
8) dL3e/dt = m2*L2*Fe*Qe – P3c*L3e – m3e*L3e
9)dL3f/dt = m2*L2*Ff*Qf – P3d*L3f – m3f*L3f
10) dL3g/dt) = m2*L2*Fg*Qg – P3g*L3g – m3g*L3g

Uninfected engorged larvae, NU1
11) dNU1/dt = m3a*L3a + m3b*L3b + m3c*L3c + m3d*L3d + m3g*L3g + (1-pL)*(m3e*L3e+m3f*L3f) – dn1*NU1-mn1*m3temp*NU1

Infected engorged larvae, NI1
12) dNI1/dt = pL*(m3e*L3e+m3f*L3f) – dn1*NI1 – mn1*m3temp*NI1

Uninfected questing nymphs, NU2
13) dNU2/dt = mn1*m3temp*NU1 – dn2*NU2 – mn2*NU2

Infected questing nymphs, NI2
14) dNI2/dt = mn1*m3temp*NI1 – dn2*NI2 – mn2*NI2

Uninfected nymphs feeding on host type a-g, FNUa-FNUg,
15) dFNUa/dt = mn2*NU2*Ga*Qa – P3f*FNUa – mfn*FNUa
16) dFNUb/dt = mn2*NU2*Gb*Qb – P3b*FNUb – mfn*FNUb
17) dFNUc/dt = mn2*NU2*Gc*Qc – P3c*FNUc – mfn*FNUc
18) dFNUd/dt = mn2*NU2*Gd*Qd – P3d*FNUd – mfn*FNUd

19) dFNUe/dt = mn2*NU2*Ge*Qe – P3c*FNUe – mfn*FNUe
20) dFNUf/dt = mn2*NU2*Gf*Qf – P3d*FNUf – mfn*FNUf
21) dFNUg/dt = mn2*NU2*Gg*Qg – P3g*FNUg – mfng*FNUg

Infected nymphs feeding on host type a-g, FNIa-FNIg,
22) dFNIa/dt = mn2*NI2*Ga*Qa – P3f*FNIa – mfn*FNIa
23) dFNIb/dt = mn2*NI2*Gb*Qb – P3b*FNIb – mfn*FNIb
24) dFNIc/dt = mn2*NI2*Gc*Qc – P3c*FNIc – mfn*FNIc
25) dFNId/dt = mn2*NI2*Gd*Qd – P3d*FNId – mfn*FNId
26) dFNIe/dt = mn2*NI2*Ge*Qe – P3c*FNIe – mfn*FNIe
27) dFNIf/dt = mn2*NI2*Gf*Qf - P3d*FNIf - mfn*FNIf
28) dFNIg/dt = mn2*NI2*Gg*Qg - P3g*FNIg - mfng*FNIg

Uninfected engorged nymph, AU1
29) dAU1/dt = mfn*(FNUa+FNUb+FNUc+FNUd)+mfng*(FNUg+FNIg)+mfn*(1-pN)*(FNUe+FNUf)-dA1*AU1-mfntemp*AU1

Infected engorged nymph, AI1
30) dAI1/dt = mfn*(FNIa+FNIb+FNIc+FNId+FNIe+FNIf) + mfn*(pN)*(FNUe+FNUf)-dA1*AI1-mfntemp*AI1

Uninfected questing adults, AU2
31) dAU2/dt = mfntemp*AU1 - dA2*AU2 - mA2*AU2

Infected questing adults, AI2
32) dAI2/dt = mfntemp*AI1 - dA2*AI2 - mA2*AI2

Uninfected adults feeding on hosts type a-g, AU3a-AU3g
33) dAU3a/dt = mA2*AU2*Ha*Qa - P3f*AU3a-mA3*AU3a
34) dAU3b/dt = mA2*AU2*Hb*Qb - P3b*AU3b-mA3*AU3b
35) dAU3c/dt = mA2*AU2*Hc*Qc - P3c*AU3c-mA3*AU3c
36) dAU3d/dt = mA2*AU2*Hd*Qd - P3d*AU3d-mA3*AU3d
37) dAU3e/dt = mA2*AU2*He*Qe - P3c*AU3e-mA3*AU3e
38) dAU3f/dt = mA2*AU2*Hf*Qf - P3d*AU3f-mA3*AU3f
39) dAU3g/dt = mA2*AU2*Hg*Qg - P3g*AU3g-mA3*AU3g

Infected adults feeding on hosts type a-g, AI3a-AI3g
40) dAI3a/dt = mA2*AI2*Ha*Qa - P3f*AI3a-mA3*AI3a
41)dAI3b/dt = mA2*AI2*Hb*Qb - P3b*AI3b-mA3*AI3b
42) dAI3c/dt = mA2*AI2*Hc*Qc - P3c*AI3c-mA3*AI3c

43) dAI3d/dt = mA2*AI2*Hd*Qd - P3d*AI3d-mA3*AI3d
44)dAI3e/dt = mA2*AI2*He*Qe - P3c*AI3e-mA3*AI3e
45) dAI3f/dt = mA2*AI2*Hf*Qf - P3d*AI3f-mA3*AI3f
46) dAI3g/dt = mA2*AI2*Hg*Qg - P3g*AI3g-mA3*AI3g

Engorged adults, A4
47)dA4/dt = mA3*(AU3a+AU3b+AU3c+AU3d+AU3e+AU3f +AU3g+AI3a+AI3b+AI3c+AI3d+AI3e+AI3f+AI3g)-dA4*A4

Host populations:

Incompetent mobile hosts (IM)
48) dIM/dt = bIM*IM*(1-IM/KIM)-dIM*IM

Incompetent stationary hosts (IS)
49) dIS/dt = bIS*IS*(1-IS/KIS)-dIS*IS

Competent uninfected mobile hosts (CUM), omitted from this simulation
50) dCUM/dt = bCUM*(CUM+CIM)*(1-(CUM+CIM)/KCM)-dCUM*CUM-Jc

Competent uninfected stationary hosts (CUS)
51) dCUS/dt = bCUS*(CUS+CIS)*(1-(CUS+CIS)./(KCS*(1+R)))-dCUS*CUS-Jd

Competent infected mobile hosts (CIM) omitted from this simulation
52) dCIM/dt = Jc-dCIM*CIM

Competent infected stationary hosts (CIS)
53) dCIS/dt = Jd-dCIS*CIS

Refractory host (WFL)
54) dWFL/dt = bWFL*WFL*(1-WFL./KWFL)-dWFL*WFL

Auxiliary equations

Total ticks on host type a-g
Ta = 0+ FNUa + FNIa + AU3a + AI3a
Tb = 0+FNUb + FNIb + AU3b + AI3b
Tc = 0+ FNUc + FNIc + AU3c + AI3
Td = 0+ FNUd + FNId + AU3d + AI3d

```
Te = 0+ FNUe + FNIe + AU3e + AI3e
Tf = 0+ FNUf + FNIf + AU3f + AI3f
Tg = 0+ FNUg + FNIg + AU3g + AI3g

On-host larvae space availability for attachment for host type a-g
Fa = max(qL*(Ca*IM-Ta)./(Ca*IM + P3a),0)
Fb = max(qL*(Cb*IS-Tb)./(Cb*IS + P3a),0)
Fc = max(qL*(Cc*CUM-Tc)./(Cc*CUM + P3a),0)
Fd = max(qL*(Cd*CUS-Td)./(Cd*CUS + P3a),0)
Fe = max(qL*(Ce*CIM-Te)./(Ce*CIM + P3a),0)
Ff = max(qL*(Cf*CIS-Tf)./(Cf*CIS + P3a),0)
Fg = max(qL*(Cg*WFL-Tg)./(Cg*WFL + P3a),0)

On-host nymph space availability for attachment for host type a-g
Ga = max(qN*(Ca*IM-Ta)./(Ca*IM + P3a),0)
Gb = max(qN*(Cb*IS-Tb)./(Cb*IS + P3a),0)
Gc = max(qN*(Cc*CUM-Tc)./(Cc*CUM + P3a),0)
Gd = max(qN*(Cd*CUS-Td)./(Cd*CUS + P3a),0)
Ge = max(qN*(Ce*CIM-Te)./(Ce*CIM + P3a),0)
Gf = max(qN*(Cf*CIS-Tf)./(Cf*CIS + P3a),0)
Gg = max(qN*(Cg*WFL-Tg)./(Cg*WFL + P3a),0)

On-host adult space availability for attachment for host type a-g
Ha = max(qA*(Ca*IM-Ta)./(Ca*IM + P3a),0)
Hb = max(qA*(Cb*IS-Tb)./(Cb*IS + P3a),0)
Hc = max(qA*(Cc*CUM-Tc)./(Cc*CUM + P3a),0)
Hd = max(qA*(Cd*CUS-Td)./(Cd*CUS + P3a),0)
He = max(qA*(Ce*CIM-Te)./(Ce*CIM + P3a),0)
Hf = max(qA*(Cf*CIS-Tf)./(Cf*CIS + P3a),0)
Hg = max(qA*(Cg*WFL-Tg)./(Cg*WFL + P3a),0)

Total number of hosts of all types
S = WFL + IM + IS + CUM + CUS + CIM + CIS

Fraction of hosts that are of type a-g, approximately
Qa = IM./(S+P3a)
Qb = IS./(S+P3a)
Qc = CUM./(S+P3a)
Qd = CUS./(S+P3a)
Qe = CIM./(S+P3a)
```

```
Qf = CIS./(S+P3a)
Qg = WFL./(S+P3a)
```

Infections in the CUM host type c compartment per day

```
Jc = pCUM*CUM.*(FNIc+AI3c)./(Tc+P3a)
```

Infections in the CUS host type d compartment per day

```
Jd = pCUS*CUS.*(FNId+AI3d)./(Td+P3a)
```

Temperature model for Mendocino

```
temp = 14.39 + -5.145*cos(t*.0172) + -5.015*sin(t*.0172) + -0.7017*cos(2*t*.0172) + 0.787* sin(2*t*.0172)
```

Daylength for Mendocino

```
LD = .5 + .125.*cos((t-174)*.0172)
```

Egg ecclosion rate

```
metemp = d3.*.0552*exp(-((temp-dfn)/ 4.946).^2).*heaviside(temp-10).*(1-heaviside(temp-tempinit)).*(heaviside(LD-LDCutN))
```

Engorged larvae maturation rate

```
m3temp = d3.*0.04001*exp(-((temp-dfn)/9.533).^2).*heaviside(temp-10).*(1-heaviside(temp-tempinit)).*(heaviside(LD-LDCutN))
```

Engorged nymph maturation rate

```
mfntemp = d3.*0.03173 *exp(-((temp-dfn)/9.042).^2).*heaviside(temp-10).*(1-heaviside (temp-tempinit))*(heaviside(LD-LDCutN))
```

Table A2: Parameter values

P3a = .001
P3b = .89
P3c = .73
P3d = .72
P3e = 2
P3f = .51
P3g = .51
pL = 0.10
pN = 0.10
Ca = 239
Cb = 176.75
Cc = 11.4
Cd = 46.84
Ce = 11.4
Cf = 46.84
Cg = 22.5
bIM = .00261
KIM = 46
dIM = .000609
mIM = 100
bIS = .0102
KIS = 45
dIS = .00129
bCUM = .00753
KCM = 3100

dCUM = .00151
mCUM = 100
pCUM = .117
bCUS = .0176
KCS = 7800
dCUS = 0.00345
pCUS = .6635
dCIM = .00151
mCIM = 100
dCIS = 0.00345
bWFL = 0.0329
KWFL =14600
dWFL = 0.000456
b = 300
de = .015
me = 1
d1 = .01
d2 =.094
d3 = 1
dn1 = .001
dn2 =.094
dfn = 20
dA1 = .001
dA2 =.094

dA3 = .01
dA4 = .5
m1 =.033
m2 = 0.5
m3a = .50
m3b = .50
m3c = .50
m3d = .50
m3e = .50
m3f = .50
m3g = .50
mn1 = 1
mn2 = .5
mfn = 0.5
mfng = 0.5
mA1 = 1
mA2 = 0.5
mA3 = .5
qL = 1
qN = 1
qA = 1
tempinit = 15
LDcutN = .45
LDcutA= 1